Chapter 4

Self Assembled Nanoscale Relaxor Ferroelectrics

Ashok Kumar, Margarita Correa, Nora Ortega,
Salini Kumari and R. S. Katiyar

Additional information is available at the end of the chapter

http://dx.doi.org/10.5772/54298

1. Introduction

Worldwide research on relaxor ferroelectric (RFE) has been carried out since 1950s. There are several schools in the world who have defined the evolution and origin of relaxor properties in the ferroelectric materials in their own way. One common consensus among the scientists is the presence of polar nano regions (PNRs) i.e. self assembled domains of short range ordering typically of less than 20-50 nm in the ferroelectric relaxor materials which causes the dielectric dispersion near the phase transition temperature. Another common approach has been also believed among the relaxor ferroelectric scientists i.e. the existence of random field at nanoscale. Random field model is considered on the experimental and theoretical facts driven from the different dielectric dispersion response under zero field cooled (ZFC) and field cooled (FC) among the relaxors.

Overall relaxor ferroelectrics have been divided into two main categories such as (i) classical relaxors (only short range ordering), the most common example is $PbMg_{1/3}Nb_{2/3}O_3$ (PMN), (ii) Semi-classical relaxor ferroelectrics (a combination of short and long range ordering). In the latter case, the relaxor properties can be arises due to compositional inhomogeneities, artificially induced strain, growth conditions (temperature, pressure, medium, etc.), and due to different ionic radii mismatched based chemical pressure in the matrix. The local domains (PNRs) reorientation induces polar-strain coupling which makes RFE the potentially high piezoelectric coefficient materials widely used in Micro/Nanoelectromechanical system (MEMS/NEMS). The basic features of the RFE over a wide range of temperatures and frequencies are as follows (i) dispersive and diffuse phase transition, (ii) partially disordered structure, (iii) existence of polar nano-ordered regions, etc. over a wide range of temperatures and frequencies. Physical and functional properties of relaxors are very different from

normal ferroelectrics due to the presence of self assembled ordered regions in the configurational disorder matrix.

This article deals with the historical development of the relaxor ferroelectrics, microstructural origin of RFE, strain mediated conversion of normal ferroelectric to relaxor ferroelectrics, superlattice relaxors, lead free classical relaxor ferroelectrics, distinction of classical relaxors and semiclassical ferroelectric relaxors based on the polarization study, and their potential applications in microelectronic industry.

2. History

Relaxor ferroelectric materials were discovered in complex perovskites by Smolenskii [1] in early fifties of twentieth centuries. Since then a vast scientific communities have been working on relaxor materials and related phenomena but the plethora of mesoscopic and microscopic heterogeneities over a range of lengths and timescales made difficult to systematic observations [2]. The microscopic image and the dielectric response of relaxor are qualitatively different for that of normal ferroelectrics. The universal signature of RFE is as follows [3 - 18]: (i) the occurrence of broad frequency-dependent peak in the real and imaginary part of the temperature dependent dielectric susceptibility (χ') or permittivity (ε') which shifts to higher temperatures with increasing frequency, G. A. Smolenskii and A. I. Agranokskaya, Soviet Physics Solid State 1, 1429 (1959), (ii) Curie Weiss law is observed at temperatures far above dielectric maxima temperature (T_m), (iii) slim hysteresis loops because polar domains are nanosized and randomly oriented, (iv) existence of polar nano domains far above T_m, (v) no structural phase transition (overall structure remains pseudo-cubic on decreasing temperature but rhombohedral-type distortion occurs in crystal at local level) across T_m in relaxors in contrast with the normal ferroelectric in which phase transition implies a macroscopic symmetry change,(vii) history dependent functional properties and skin effects (surface behavior is quite different than the interior of the system) (vi) in most cases, relaxor crystal showed no optical birefringence (either far below the freezing temperature and/or under external electric field).

As we know ferroelectric and related phenomenon are synonyms of ferromagnetism, antiferromagnetism, spin glass, and random field model which have been originally studied for magnetic materials. Relaxors ferroelectrics possess a random field state, as initially proposed by Westphal, Kleemann and Glinchuk [16-18]. Near Burns temperature, small polar nano regions start originating in different directions inside the crystal at mesoscopic scale; however, these polar nano regions are not static in nature at Burns temperature. At low temperature these polar nanoregions (PNRs) become static and developed a more defined regions called random field, the nature of these fields are short range order. The evidence of the existence of nanosized polar domains at temperatures well above the dynamic transition temperature comes for experimental observations. The presence of these polar nanoregions (PNRs) was established by measuring properties that depend on square of the polarization (P^2) and by direct imaging with TEM studies. The first evidences came from a report by Burns and Da-

col [5] who studied the electro-optical effect in a PMN crystal. In case of normal FE, the temperature dependence of the refraction index *(n)* show a linear decrease of n from the paraelectric phase down to phase transition temperature (T_c), below T_c n deviates from linearity. The deviation is proportional to the P^2 and it increases as the polarization changes with temperature. Burns and Dacol observed deviation from linear $n(T)$ in relaxor PMN crystal well above T_m, the onset of the deviation was observed at 620 K, almost 350 K above T_m. The temperature in which onset of deviation from linearity of $n(T)$ occurs (in any relaxor) had been identified in the literature as the Burns temperature (T_B or T_d).

Electrostriction is a property which depends on P^2. Thermal strain in a cubic perovskite has two components, one due to the linear coefficient of thermal expansion, α, and another due to electrostriction accounted by the electrostrictive coefficients Q_{ijkl}. Measures on the temperature dependence of thermal expansion in RFE crystals have shown that the contribution due to electrostriction vanishes only above T_B where P=0.

The existence of PNRs well above T_m and the growth of these domains with decreasing temperature have been demonstrated by TEM [8 - 12]. Transmission electron studies also account for the B-cation order in complex perovskites [11 - 12]. Ordering of the B-site cations occurs if there is sufficiently large interaction energy between neighboring cations.

3. Theory of relaxor ferroelectricity

The general formula of perovskite having A and B-site cations with different charge states can be written as $A'_xA''_{1-x}B'_yB''_{1-y}O_3$. The randomness occupancy of A′,A′′ and B′,B′′ in A, B site respectively, depends on the ionic sizes, distribution of cations ordering at sub lattices and charge of cations. If the charges of cations at B-sites are same it is unlikely to have the polar randomness at nanoscale. Long range order (LRO) is defined as a continuous and ordered distribution of the B cations on the nearest neighbor sites. The short coherence length of LRO occurs when the size of the ordered domains are in a range of 20 to 800 Å in diameter. The long coherence range of LRO occur when the size of the ordered domains are much greater than 1000 Å. Randall et al. made a classification of complex lead perovskite and their solid solutions based on B-cation order studied by TEM and respective dielectric, X-rays and optical properties [11]-[12]. This classification divides the complex lead perovskites into three subgroups; random occupation or disordered, nanoscale or short coherent long-range order and long coherent long-range order of B-site cations.

Diffuse phase transition behavior is characteristic of the disordered structures. In these structures, random lattice disorder introduces dipolar impurities and defects that influence the static and dynamic properties of these materials. The presence of the dipolar entities on a lattice site of the highly polarizable FE structure, induced dipoles in a region determined by the correlation length (r_c). The correlation length is a measure of the extent of dipoles that respond in a correlated manner. In normal FE, r_c is larger than the lattice parameter *(a)* and it is strongly temperature dependent. On decreasing the temperature, a faster increase of r_c promotes growing of polar domains yielding a static cooperative long-range ordered FE

state at $T < T_c$. This is not the case for RFE where a small correlation length of dipoles leads to formation of polar nanodomains frustrating the establishment of long-range FE state. Therefore, the dipolar nanoregions form a dipolar-glass like or relaxor state at low temperature with some correlation among nanodomains.

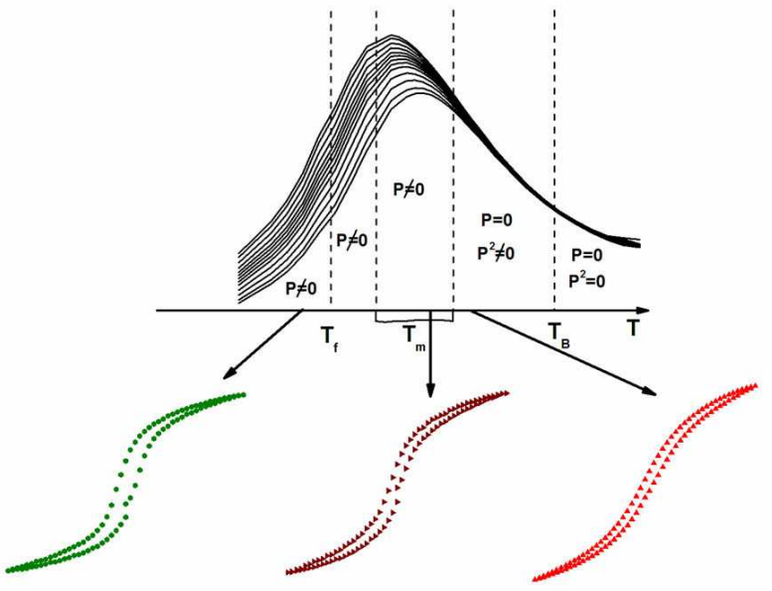

Figure 1. Temperature evolution of dielectric constant showing the characteristic temperatures in RFE. Representative hysteresis loops for each temperature interval are showed below.

These PNRs are dynamic and they experience a slowing down of their fluctuations at $T \leq T_m$. The dielectric relaxation does not fit the classical Debye relaxation model; instead there is a distribution of relaxation times related to the sizes of the nanodomains. The temperature dependence of dielectric constant as shown in Fig. 1 indentifies the main temperatures associated with relaxor ferroelectric behavior. These temperatures are T_B, T_m and T_f, we already defined T_B and T_m but the definition of T_f follow from the fit of the frequency dispersion of T_m with the Vogel-Fulcher law [15]. The dynamics of polar nanoregions does not follow Arrhenius type temperature dependence; instead nice fit of the frequency dispersion for each relaxor system is obtained with the Vogel-Fulcher law:

$$f = f_0 exp\left(\frac{-E_a}{k_B(T_m - T_f)}\right) \tag{1}$$

where f_0 is the attempt frequency which is related to the cut-off frequency of the distribution of relaxation times, E_a is the activation barrier to dipole reorientation, T_m is the dielectric maxima temperature, and T_f is the freezing temperature where polarization fluctuations "frozen-in".

http://dx.doi.org/10.5772/54298

The temperature dependence of the dielectric constant below T_B and in the vicinity of T_m is normally fitted by the empirical power law [19]:

$$\frac{1}{\varepsilon(\omega,\ T)} = \left(\frac{1}{\varepsilon_{max}(\omega,\ T)}\right)\left(1 + \frac{(T - T_{max})^{\gamma}}{2\delta^2}\right) \tag{2}$$

where γ and δ are parameters describing the degree of relaxation and diffuseness of the transition respectively. The parameter γ varies between 1 and 2, where values closer to 1 indicate normal ferroelectric behavior whereas values close to 2 indicate good relaxor behavior. Above T_B the inverse of dielectric permittivity is fitted by the Curie-Weiss law:

$$\chi = \frac{C}{T - \Theta} \tag{3}$$

where C and Θ are the Curie constant and Curie temperature respectively.

Last sixty years of extensive research in the field of relaxor ferroelectrics, several models have been proposed to explain the unusual dielectric behavior of these materials. Some of these models are: statistical composition fluctuations [20, 21], superparaelectric model [22], dipolar glass model [23], random field model [24], spherical random field model [25] etc. These models can explain much of the experimental observed facts but a clear understanding of the relaxor nature or even a comprehensive theory is not available yet. Despite the absence of a comprehensive theory of relaxor ferroelectricity, the literature agree to define relaxor materials in terms of the existence of polar nano regions as motioned above, these ordered regions exist in a disordered environment.

4. Strain induced relaxor phenomenon

The influence of epitaxial clamping on ferroelectric properties of thin films to rigid substrates has been largely studied and successfully explained in a Landau-Ginzburg-Devonshire (LGD) framework [26-30]. However, when the same treatment was applied to RFE, discrepancies among the predicted values and those observed in experiments were found [30]. For instance, a downward shift in T_m of PMN films in the presence of compressive in-plane strain was found, contrary to the expected upward shift. Catalan [30] et al. developed a model to analyze the influence of epitaxial strain on RFE. This model is based on LGD theory but assuming a quadratic dependence on (T-T_m), rather than linear, for the first coefficient of the free energy. Catalan's model shows that the shift in T_m for relaxors thin films do not depend on the sign of the epitaxial mismatch strain, but rather on the thermal expansion mismatch between substrate and film. Reference [30] also provided a list of compounds which exhibited shift in T_m when they were grown in film forms. We have already observed in-plane strain in our $Pb(Sc_{0.5}Nb_{0.25}Ta_{0.25})O_3$(PSNT)/$La_{0.5}Sr_{0.5}CoO_3$ (LSCO)/MgO heterostructure, which may have caused the measured shift of T_m with respect to bulk values [31-33].

We have calculated shift in the peak position of the dielectric maxima of PSNT films compared to bulk values following the model developed by Catalan et.al. The model is as follow: In LGD formalism, the thermodynamical potential of a perovskite dielectric thin films is described as [27-28].

$$\Delta G = \left(\frac{1}{2}\alpha - Q_{i3}X_i\right)P_3^2 + \frac{1}{4}\beta P_3^2 - \frac{1}{2}s_{ij}\left(X_i X_j\right) \tag{4}$$

where α and β correspond to linear and nonlinear terms of the inverse permittivity, and s_{ij}, X_i, and Q_{i3} are the elastic compliances, the stress tensor, and the electrostriction tensor in Voigt notation; P_3 is out of the plane polarization. Strain gradients across the films are neglected. The inverse permittivity is the second derivative of the free energy with respect to the polarization:

$$\chi_3^{'} = \frac{\partial^2 \Delta G}{\partial P^2} = \alpha - 4Q_{13}\frac{Y}{1-\nu}x_m + 3\beta P_3^2 \tag{5}$$

where x_m, Y, and ν are the mismatch strain, Young's modulus, and Poisson's ratio of the film respectively. For conventional ferroelectrics, α is usually expanded in a power series of $(T\text{-}T_c)$:

$$\alpha = \frac{1}{C\varepsilon_0}\left(T - T_c\right) + f\left(T - T_c\right)^2 \tag{6}$$

which directly leads to Curie-Weiss behavior, where C is the Curie constant. Substituting α into the above equation showing that the strain shifts the critical temperature for a ferroelectric by:

$$\Delta T_c = 4C\varepsilon_0 Q_{13}\frac{Y}{1-\nu}x_m \tag{7}$$

Since Q_{13} is always negative, it has been observed that the shift in the critical temperature depends on the sign of in-plain strain: T_c decreases for the tensile strain and it increases for compressive strain. Equation 7 is not adequate to explain the shifts in the dielectric maximum temperature for the relaxor ferroelectric materials

In case of PSNT films, we observed a quadratic temperature dependence of the permittivity:

$$\frac{1}{\varepsilon(\omega, T)} - \frac{1}{\varepsilon_m(\omega, T)} = \frac{1}{2\varepsilon_m\varepsilon_0}\left(T - T_m\right)^2 \tag{8}$$

Since the inverse of the dielectric constant is the second derivative of free energy with respect to polarization (Equation 5), the measured dielectric constant can be related to the appropriate coefficients in the LGD thermodynamical potential. For P=0 and x_m=0 (in the absence of strain), χ correlates with the first coefficient of the Landau equation, i.e.

$$\chi(T, f)=\alpha(T, f)=\frac{1}{2\varepsilon_m\varepsilon_0}(T - T_m)^2 \tag{9}$$

We substituted the values of α in Equation 5 and calculated the dielectric maxima temperature under strain $(T_m^{'})$. To calculate $T_m^{'}$, we differentiated the inverse of permittivity with respect to temperature at $T_m^{'}$.

$$\frac{\partial \chi^{'}}{\partial T_m^{'}}=0=\frac{1}{\varepsilon_0\varepsilon_m\delta^2}\left(T_m^{'} - T_m\right) - 4Q_{13}\frac{Y}{1 - \nu}\frac{\partial x_m}{\partial T} \tag{10}$$

where it is assumed that Q_{13}, Y, and ν do not change substantially [34] with temperature in the dielectric maxima regions; only the mismatch strain changes due to differential thermal expansion:

$$\frac{\partial x_m}{\partial T}=\frac{\partial}{\partial T}\left[\frac{\left(a_{film}\left[1 - \lambda_{substrate}(T - T_0)\right] - a_{bulk}\right)}{a_{bulk}}\right] \tag{11}$$

where $\lambda_{substrate}$ is the coefficient of thermal expansion of the substrate, a_{film} and a_{bulk} are the lattice constant of the film and the bulk respectively. Using Equations, 9, 10, and 11 the expected shift in T_m is:

$$\Delta T_m=4\delta^2\varepsilon_m\varepsilon_0 Q_{13}\frac{Y}{1 - \nu}\frac{a_{film}}{a_{bulk}}\lambda_{substrate} \tag{12}$$

We have used the above equation to calculate the shift in the position of dielectric maxima of PSNT films. Due to lack of experimental mechanical data in literature for PSNT films or ceramics, we have used the standard Q_{13} for PST thin films [34] and Y value for the PMN single crystal [35] other values we got from our experimental observation i.e. (δ, ε_m, a_{film}, a_{bulk}). For MgO substrate, $\lambda_{substrate} = 1.2\text{x}10^{-5}$ K^{-1}. Putting all these data in Equation 12 we got a shift in the dielectric maximum temperature (T_m) of the same magnitude order than those of experimental observation.

5. Experimental observation of strain induced relaxor phenomenon

Fig. 2 shows the dielectric behavior and the microstructures of the PSNT thin films and their bulk matrix [31-33]. It has been shown that the two-dimensional (2D) clamping of films by the substrate may change profoundly the physical properties of ferroelectric heterostructure with respect to the bulk material. We observed a transfer and relaxing of epitaxial strain between the layers due to in-plane oriented heterostructure. However the mismatch strain due to different thermal expansion properties of each layer provokes a shift of 62 K in the temperature of the dielectric maxima.

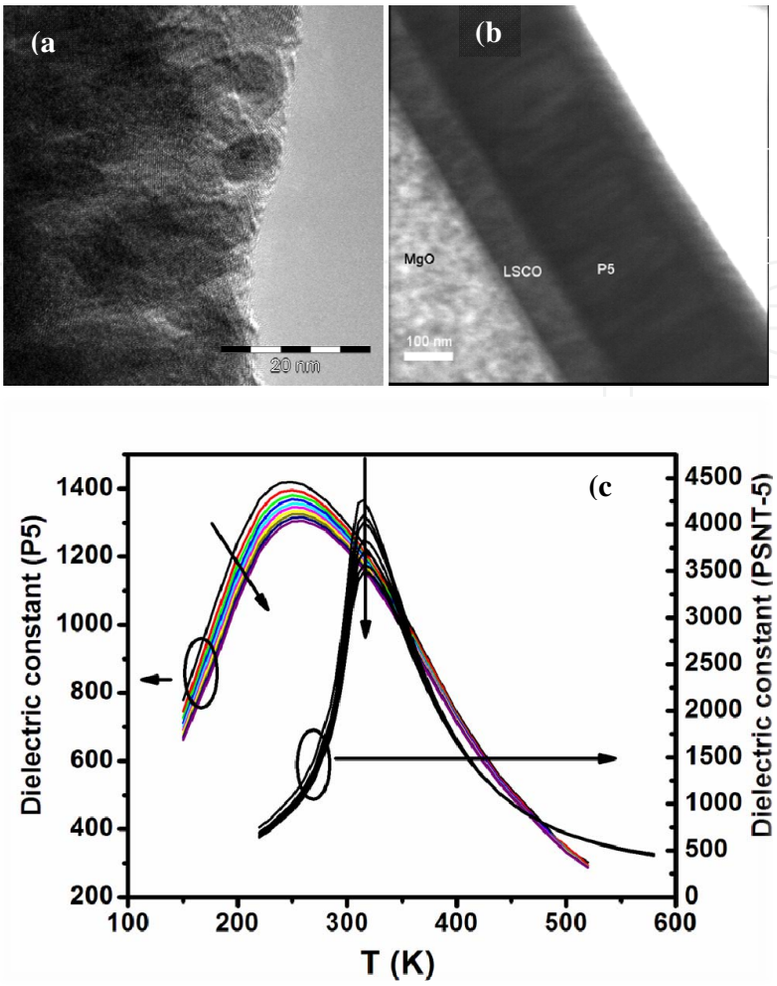

Figure 2. Microstructure of the PSNT bulk nanoceramics (a) and the thin films (b) grown on the LSCO coated MgO substrate, and a drastic shift in dielectric maxima temperature (c) in PSNT thin film with respect same compositions of their bulk counterpart. The microstructures of film and ceramic support the existence of strain induced relaxor phenomenon, as their microstructures- property correlation indicate the presence of some ordered polar nano-regions in the thin films whereas absence of such effect in bulk. Figure 2(a) was adapted from Ref. [31] and reproduced with permission (© 2008 John Wiley and Sons).

Transmission electron microscopy (TEM) images of PSNT in bulk (Fig. 2(a)) and thin film (Fig. 2(b)) form are shown in Fig. 2. The interlayer of about 20 nm between MgO and LSCO and the fibril structures along a single direction in the film confirm the in-plane strain state of the film. TEM image of bulk shows well ordered nanoregions in the grain matrix that meet a basic ingredient to produces relaxor behavior: the existence of nano-ordered regions surrounding by a disordered structure, however, it is unable to produce it. It has been observed from the neutron diffraction data that if the ordered nanoregions are in the range of ~ 5-10 nm, then it is capable of yielding frequency dispersion in the dielectric spectra [30]. But the relaxor state also depends on the coherency with what the dipoles respond to the probing field (and frequency). They can establish long range or short range coherent response. PSNT ceramic was incapable to produce the frequency dispersion behavior, but in thin films form the in plane strain and the breaking of long range or-

http://dx.doi.org/10.5772/54298

dering response, induced dielectric dispersion and shifting in dielectric maxima temperature towards lower temperature side. We have observed from the temperature evolution of the Raman spectra of bulk PSNT ceramic [31-33], the competitions between ordered domains of short and long-range order due to Nb- and Ta-rich regions respectively. The average disorder arrangement of $Sc^{3+}/Nb^{5+}/Ta^{5+}$ ions in the B-site octahedra leads to the observed diffuse phase transition. In film only short range ordering in B'/B'' ions was developed within the disordered matrix. Although bulk matrix exhibited nano-ordered regions its average size must be higher than film. Stress effects change the ionic positions somehow favoring short-range ordering. These microstructural differences trigger the different observed dielectric responses. The microstructure-property relation of PSNT thin films and ceramics, one can build conclusions that perovskite with similar compositions have well defined relaxor behavior than their bulk matrix.

6. Birelaxors

We have discussed the origin and functional properties of relaxor, in nutshell the basic characteristic of relaxors are the existence of ordered PNRs in a disordered matrix [37-42]. Similarly, relaxor ferromagnets (synonyms: "Mictomagnets") are also known in the literature since the 1970s. A mictomagnet is described as having magnetic clusters (superparamagnetism) which form a spin glass and have a tendency to form short-range ordering [40, 41]. The materials hold both ferroelectric and magnetic orders at nanoscale are called "birelaxors". Birelaxors are suppose to possess only short range order over the entire temperature range with broken symmetry such as "global spatial inversion" and "time reversal symmetry" at nanoscale. Nanoscale broken symmetries and length scale coherency make birelaxors difficult to investigate microscopically; it is advisable to use optical tools for proper probing. Birelaxors do not usually show linear ME coupling ($a_{ij}\ P_i\ M_j$) but may have large nonlinear terms such as bP^2M^2. Since linear coupling is not allowed, local strain-mediated PNR-PNR, PNR-MNR (magnetic nanoregions), and MNR-MNR interactions may provide very strong ME effects [43-44].

A single-phase perovskite $PbZr_{0.53}Ti_{0.47}O_3$ (PZT) and $PbFe_{2/3}W_{1/3}O_3$ (PFW), (40% PZT-60 % PFW) solid solutions thin film grown by pulsed laser deposition system have shown interesting birelaxor properties. Raman spectroscopy, dielectric spectroscopy and temperature-dependent zero- field magnetic susceptibility indicate the presence of both ferroic orders at nanoscale [45].

Dipolar glass and spin glass properties are confirmed from the dielectric and magnetic response of the PZT-PFW system, the micro Raman spectra of this system also revealed the presence of polar nanoregions. Dielectric constant and tangent loss show the dielectric dispersion near the dielectric maxima temperature that confirms near-room-temperature relaxor behavior. Magnetic irreversibility is defined as ($M_{irr}= M_{FC}-M_{ZFC}$) and it represents the degree of spin glass behavior. PZT-PFW demonstrates special features in M_{irr} data at 100 Oe indicate that irreversibility persists above 220 K up to 4^{th} or 5^{th} order of the magnitude, T_{irr} (inset Fig. 3 (b)). The evidence of ZFC and FC splitting at low field ~100 Oe and

even for high 1 kOe field suggests and supports glass-like behavior with competition between long-range ordering and short-range order. The behavior of the ZFC cusp is the same for the entire range of field (>100 Oe), with a shift in blocking transition temperature (T_B) (maximum value of magnetization in ZFC cusp) to lower temperature, i.e. from 48 K to 29.8 K with increasing magnetic field. The ZFC cusps disappeared in the FC process, suggesting that competing forces were stabilized by the field- cooled process. Magnetic irreversibilities were found over a wide range of temperature with a sharp cusp in the ZFC data, suggesting the presence of MNRs with spin-glass-like behavior. The detailed fabrication process, the complete characterization process and the functional properties are reported in reference [43]. This is not only the unique system to have birelaxor properties, however, Levstik et al also observed the birelaxor properties in $0.8Pb(Fe_{1/2}Nb_{1/2})O_3$–$0.2Pb(Mg_{1/2}W_{1/2})O_3$ thin films [38].

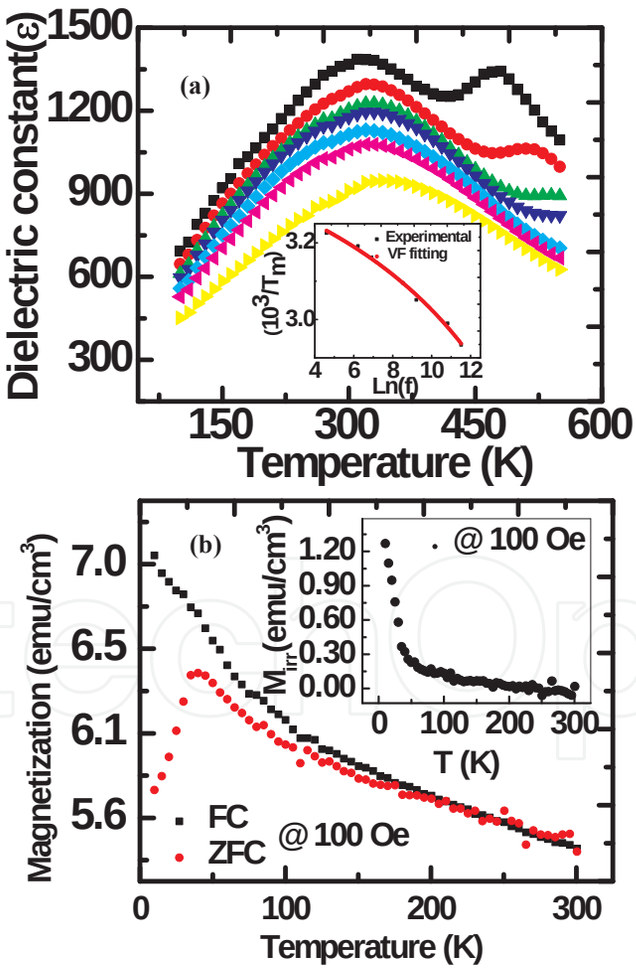

Figure 3. (a) Dielectric response and Vogel-Fulcher fitting (inset), (b) Zero field cooled and field cool magnetic response of PZT-PFW thin films indicate the presence of PNRs and MNRs at nanoscale. Adapted from Ref. [45] and reproduced with permission (© 2011 AIP).

7. Superlattice relaxors and high energy density capacitors

Material scientists are looking for a system or some novel materials that possess high power density and high energy density or both. Relaxors demonstrate high dielectric constant, low loss, non linear polarization under external electric field, high bipolar density, nano dipoles (polar nano regions (PNRs) and moderate dielectric saturation, these properties support their potential candidature for the high power as well as high energy devices. At present high-k dielectric (dielectric constant less than 100, with linear dielectric) dominates in the high energy, high power density capacitor market. The high-k dielectrics show very high electric breakdown strength (> 3 MV/cm to 12 MV/cm) but their dielectric constant is relatively very low which in turns offer 1-2 J/cm^3 volume energy density. Recently, polymer ferroelectric, antiferroelectric, and relaxor ferroelectric have shown better potential and high energy density compare to the existing linear dielectrics [46-51].

$BaTiO_3/Ba_{0.30}Sr_{0.70}TiO_3$ (BT/BST) superlattices (SLs) with a constant modulation period of Λ= 80 Å were grown on (001) MgO substrate by pulsed laser deposition. The modulation periodicity $\Lambda/2$ was precisely maintained by controlling the number of laser shots; the total thickness of each SL film was ~6,000 Å = 0.6 μm. An excimer laser (KrF, 248 nm) with a laser energy density of 1.5 J/cm^2, pulse repetition rate of 10 Hz, substrate temperature 830 °C, and oxygen pressure at 200 mTorr was used for SL growth. The detailed growth and characterization techniques are presented elsewhere [52].

Dielectric responses of BT/BST SLs display the similar response as for normal relaxor ferroelectric which can be seen in Figure 4. It follows the non linear Vogel- Fulcher relationship (inset Figure. 4 (a)), frequency dispersion near and below the dielectric maxima temperature (T_m), merger of frequency far above the T_m, shift in T_m towards higher temperature side (about 50-60 K) with increase in frequencies, low dielectric loss, and about 60-70% dielectric saturation.

BT/BST SLs demonstrate a "in-built" field in as grown samples at low probe frequency (<1 kHz), whereas it becomes more symmetric and centered with increase in probe frequency system (>1 kHz) that ruled out the effect of any space charge and interfacial polarization. Energy density were calculated for the polarization-electric field (P-E) loops provide ~ 12.24 J/cm^3 energy density within the experimental limit, but extrapolation of this data in the energy density as function of applied field graph for different frequencies (see inset in Figure 4) suggests huge potential in the system such as it can hold and release more than 40 J/cm^3 energy density.

Experimental limitations restrict to proof the extrapolated data, however the current density versus applied electric field indicates exceptionally high breakdown field (5.8 to 6.0 MV/cm) and low current density (~ 10-25 mA/cm^2) near the breakdown voltage. Both direct and indirect measurements of the energy density indicate that it has ability to store very high energy density storage capacity (~ 46 J/cm^3).

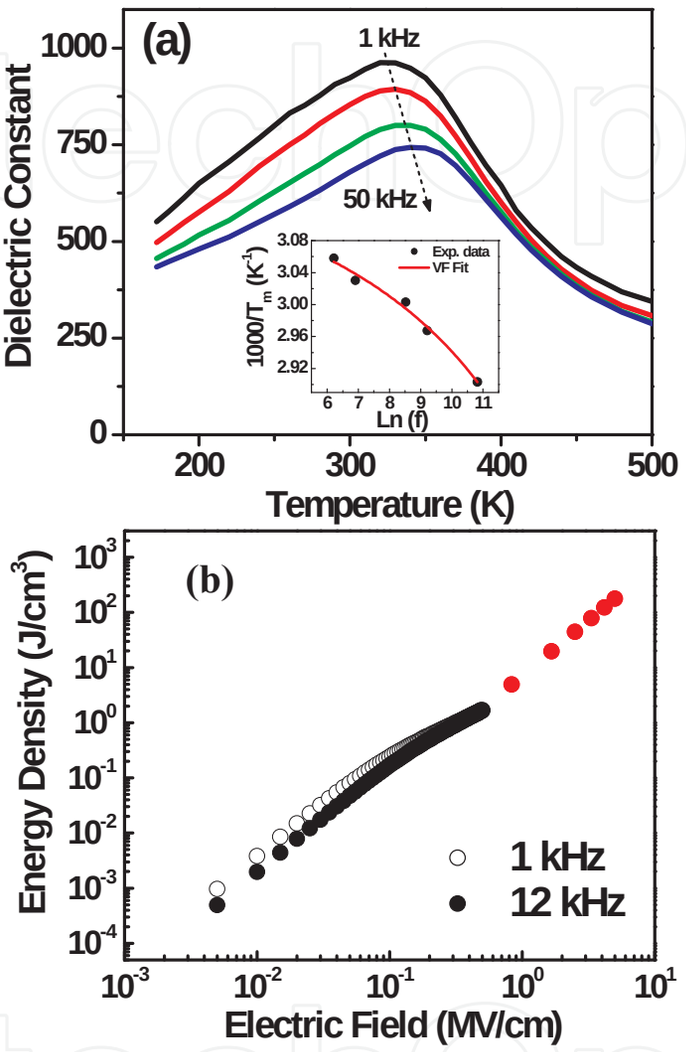

Figure 4. (a) Dielectric responses of BT/BST superlattice relaxors as function of temperature over wide range of frequencies, nonlinear Vogel-Fulcher relationship (inset), (b) Energy density capacity as function of applied electric filed, red dots show the extrapolated data. Adapted from Ref. [46] and reproduced with permission (© 2012 IOP).

The above experimental facts suggest the relaxor nature of BT/BST ferroelectric superlattices. It also indicates their potential to store and fast release of energy density which is comparable to that of high-k (<100) dielectrics, hopefully in the coming years it might be suitable for high power energy applications. These functional properties of relaxor superlattices make it plausible high energy density dielectrics capable of both high power and energy density applications.

8. Conclusions

Extensive studies on the relaxor ferroelectrics suggest the presence of localized nano size ordered regions in the disordered matrix or static random field are responsible for the dielectric dispersion near T_m. The nano regions and their coherence length are also critical for the relaxor behavior. A normal ferroelectric with diffuse phase transition system can be turn to relaxor ferroeletrics in their thin film forms under the suitable applications of strain, utilizing highly lattice mismatch substrate, growth conditions (thermal, oxygen partial pressure, atmosphere), etc.. It also indicates that the defects, oxygen vacancies, ordering of cations at A and B site of perovskite, tensile or comprehensive strain across the interface, etc. originate the ordered nano regions in films mainly responsible for dielectric dispersion. Materials with same compositions can have normal ferroelectric in bulk form whereas become relaxor in the thin film. Birelaxors hold both ferroics orders at nano scale with only short range ordering (SRO). These nanocale SRO make it potential candidates for non linear biquadratic magneto-electric coupling suitable for magnetic field sensors and non volatile memory applications. BT/BST superlattice has shown very high dielectric constant, high breakdown field, relaxor, and high energy density functional properties. A Relaxor superlattice with high functional properties is capable for both high power and energy density applications.

Acknowledgement

This work was partially supported by NSF-EFRI-RPI-1038272 and DOE-DE-FG02-08ER46526 grants.

Author details

Ashok Kumar[1,2], Margarita Correa[2], Nora Ortega[2], Salini Kumari[2] and R. S. Katiyar[2]

*Address all correspondence to: ashok553@gmail.com

1 National Physical Laboratory, Council of Scientific and Industrial Research (CSIR), New Delhi, India

2 Department of Physics and Institute for Functional Nanomaterials, University of Puerto Rico, San Juan, Puerto Rico

References

[1] G. A. Smolenskii and A. I. Agranokskaya, Soviet Physics Solid State 1, 1429 (1959)

[2] R. E. Cohen, Nature, 441, 941 (2006)

[3] Eric Cross, Ferroelectrics, 151, 305, (1994)

[4] G. A. Samara, J. Phys.: Condens. Matter 15, R367, (2003)

[5] G. Burns and F. H. Dacol, Solid State Communications, 48, 853, (1983)

[6] G. A. Samara, Solid State Physics, vol. 56, Edited by H. Ehrenreich, and R. Spaepen, New York: Academic, New York (2001)

[7] B. Krause, J. M. Cowley, and J. Wheatly, Acta Cryst. A35, 1015 (1979)

[8] C.A. Randall, D. J. Barber, and R. W. Whatmore, J. Micro. 145, 235 (1987)

[9] J. Chen, H. Chen, and M. A. Harmer, J. Am. Ceram. Soc. 72, 593 (1989)

[10] I. M. Brunskill, H. schmid, and P. Tissot, Ferroelectrics 37, 547 (1984)

[11] C. A. Randall, A. S. Bhalla, T. R. Shrout, and L. E. Cross, J. Mater. Res., 5, 829 (1990)

[12] C. A. Randall and A. S. Bhalla, Japanese Journal of Applied Physics, 29, 327 (1990)

[13] Ferroelectrics and Related Materials, G. A. Smolenskii (Ed.), V. A. Bokov, V. A. Isupov, N. N. Krainik, R. E. Pasynkov and A. I. Sokolov, Gordon & Breach Science Publisher, New York (1984)

[14] Z.-G Ye, Key Engineering Materials, 155-156, 81 (1998)

[15] H. Vogel. Z. Phys. 22, 645 (1921). G. Fulcher. J. Am. Ceram. Soc. 8, 339 (1925)

[16] V.Westphal,W. Kleeman, and M.D. Glinchuk, Phys. Rev. Lett. 68, 847 (1992).

[17] R. Pirc and R. Blinc, Phys. Rev. B. 60, 13470 (1999).

[18] R. Blinc, J. Dolinsek, A. Gregorovic, B. Zalar, C. Filipic, Z. Kutnjak, A. Levstik, and R. Pirc, Phys. Rev. Lett. 83, 424 (1999).

[19] H.T. Martirena and J.C. Burfoot. Ferroelectrics, 7, 151 (1974)

[20] G. A. Smolenskii, V. A. Isupov, A. I. Agranovskaya and S. N. Popov, Soviet Phys.-Solid State. 2, 2584 (1961).

[21] G. A. Smolenskii, J. Phys. Soc. Jpn. 28, Suppl. 26 (1970).

[22] L.E. Cross, Ferroelectrics 76, 241 (1987).

[23] D. Viehland, J. F. Li, S. J. Jang, and L. E. Cross and M. Wuttig. Phys. Rev. B. 43, 8316 (1991).

[24] R. Fisch. Phys. Rev. B. 67, 094110 (2003).

[25] R. Pirc and R. Blinc, Phys. Rev. B. 60, 13470 (1999)

[26] F. Devonshire, Philos. Mag. 40, 1040, (1949); 42, 1065, (1951)

[27] G.A. Rossetti Jr., L.E. Cross, and K. Kushida, Appl. Phys. Lett., 59, 2504 (1991)

[28] N.A. Perstev, A.G. Zembilgotov, and A. K. Tagantsev, Phys. Rev. Lett., 80, 1988 (1998)

[29] M. Dawber, K.M. Rabe, and J.F. Scott, Reviews of Modern Physics, 77, 1083, (2005)

[30] G. Catalan, M. H. Corbett, R. M. Bowman, and J. M. Gregg, J. App. Phys., 91, [4] 2295 (2002).

[31] Margarita Correa, A. Kumar and R.S. Katiyar, J. Am. Cer. Soc. 91 (6) 1788 (2008).

[32] Margarita Correa, Ashok Kumar, and R. S. Katiyar, Applied Physic Letters, 91, 082905 (2007).

[33] Margarita Correa, Ashok Kumar, and R. S. Katiyar, Integrated Ferroelectrics, 100, 297 (2008)

[34] K. Brinkman, A. Tagantsev, P. Muralt, and N. Setter, Jpn. J. App. Phys., 45, [9B] 7288 (2006)

[35] Q.M. Zhang and J. Zhao, Appl. Phys. Lett., 71, 1649 (1997)

[36] D. L. Orauttapong, J. Toulouse, J. L. Robertson, and Z. G. Ye, Physical Rev. B , 64, 212101 (2001).

[37] A. Kumar, N. M. Murari, and R. S. Katiyar, Appl. Phys. Lett. 90, 162903 (2007).

[38] A. Levstik, V. Bobnar, C. Filipič, J. Holc, M. Kosec, R. Blinc, Z. Trontelj, and Z. Jagličič, Appl. Phys. Lett. 91, 012905, (2007).

[39] V. V. Shvartsman, S. Bedanta, P. Borisov, W. Kleemann, A. Tkach, and P. M. Vilarinho, Phys. Rev. Lett. 101, 165704 (2008).

[40] G. A. Samara, in Solid State Physics, edited by H. Ehrenreich and R. Spaepen Academic, New York, 2001, Vol. 56, p. 239.

[41] J. Dho, W. S. Kim, and N. H. Hur, Phys. Rev. Lett. 89, 027202 (2002).

[42] R. Pirc and R. Blinc, Phys. Rev. B 76, 020101R (2007).

[43] A. Kumar, G. L. Sharma, R. S. Katiyar, R. Pirc, R. Blinc, and J. F. Scott, J. Phys.: Condens. Matter 21, 382204 (2009).

[44] R. Pirc, R. Blinc, and J. F. Scott, Phys. Rev. B 79, 214114 (2009).

[45] A. Kumar, G. L. Sharma, R. S. Katiyar, Appl. Phys. Lett. 99, 042907 (2011).

[46] J. H. Tortai, N. Bonifaci, A. Denat, J. Appl. Phys. 97, 053304 (2005).

[47] M. Rabuffi, G. Picci, IEEE Trans. Plasma Sci. 30, 1939 (2002).

[48] X. Hao, J. Zhai, and, X. Yao, J. Am. Ceram. Soc., 92, 1133 (2009).

[49] J. Parui, S. B. Krupannidhi, Appl. Phys. Lett., 92, 192901 (2008).

[50] R. M. Wallace, G. Wilk, MRS Bulletin. 27, 186 (2002).

[51] G. D. Wilk, R. M. Wallace, J. M. Anthony, J. Appl. Phys. 89, 5243 (2001).

[52] N. Ortega, A Kumar, J. F. Scott, Douglas B. Chrisey, M. Tomazawa, Shalini Kumari, D. G. B. Diestra and R. S. Katiyar. J. Phys.: Condens. Matter. 24 445901 (2012).